On the outage performance of line-of-sight massive MIMO with a fixed-length uniform linear sparse array

On The Outage Performance Of Line-Of-Sight Massive MIMO with a Fixed-Length Uniform Linear Sparse Array

A. Farsaei*, N. Amani†, A. Alvarado*, F. M. J. Willems*, U. Gustavsson‡, R. Maaskant*†

*Eindhoven University of Technology, Eindhoven, The Netherlands,
†Chalmers University of Technology, Gothenburg, Sweden,
‡Ericsson Research, Gothenburg, Sweden

***Abstract*—Increasing the inter-element spacing of a uniform linear sparse array results in reducing the mutual coupling and simplifying the heat dissipation control of the array. However, increasing the inter-element spacing may result in the appearance of grating lobes in the field-of-view (FoV). In this paper, 0.05-outage capacity is used as the performance metric to optimize the inter-element spacing for a given array size in line-of-sight scenarios. For the case of two users, we propose to increase the inter-element spacing as long as the 0.05-outage capacity does not reduce more than 1% compared to the capacity achieved when the two users have orthogonal channel vectors. Radiated power at the base station is adjusted to have the same effective isotropic radiated power for different arrays. Simulation results for an array size of 40λ show that for FoVs of 60° to 120°, the inter-element spacing can be increased from 0.5λ to more than 1.14λ.**

***Index Terms*—Line-of-sight, outage, uniform linear sparse array.**

I. Introduction

Massive MIMO is a promising technology for 5G wireless networks, which provides high data throughput and radiated-energy efficiency [1]. Analyzing line-of-sight (LOS) propagation environments is crucial since the real propagation environment is likely to fall between LOS and independent and identically distributed (i.i.d.) Rayleigh [2]. Moreover, "open exhibition" and "crowded auditorium" are mentioned in [3] for which the channel vectors from the base station (BS) to the users are often LOS.

Increasing the inter-element spacing between the elements at the BS results in a reduced mutual coupling among the elements and simplifies the heat dissipation control of the array [4]. However, increasing the inter-element spacing may result in the appearance of grating lobes in the field-of-view (FoV). The grating lobes may cause a high inter-user interference, which degrades the communication, and drives the system into an outage. To avoid the appearance of grating lobes for an array with a fixed number of elements, [5] proposed to increase the inter-element spacing while limiting the FoV. In this way, the grating lobes are suppressed with the assumption of low radiation outside the FoV. In [6], [7], fixed-length arrays are studied from different aspects for i.i.d. Rayleigh fading channel. However, the effects of grating lobes on communication for fixed-length arrays have to be further studied for LOS scenarios.

In this paper, the effects of grating lobes are addressed by studying the outage performance as a function of inter-element spacing and FoV employing fixed-length sparse arrays in LOS environments. We use the outage performance as the performance metric to optimize the inter-element spacing for a given FoV. The optimization is done for the case of two users uniformly distributed in the FoV at the cell-edge. We propose to increase the inter-element spacing as long as the outage performance does not reduce more than 1% compared to the capacity achieved when the users have orthogonal channel vectors. In our analysis, the radiated power is adjusted for different arrays to have the same effective isotropic radiated power (EIRP).

This project has received funding from the European Union's Horizon 2020 research and innovation programme under the Marie Sklodowska-Curie grant agreement No 721732.

II. System Model

The model for the downlink channel from an M-antenna BS to K single-antenna users is shown in Fig. 1[1]. The transmitted vector $\boldsymbol{x} \in \mathbb{C}^{M\times 1}$ from a uniform linear sparse array at the BS goes through the channel $\boldsymbol{H} = (\boldsymbol{h}_1, ..., \boldsymbol{h}_K)^T \in \mathbb{C}^{K\times M}$, where $\boldsymbol{h}_i$ is the channel vector from the BS to user i. In LOS environments, the element ij of the channel matrix denoted by h_{ij} is modeled by [8, Sec. 7.2.2]:

$$h_{ij} = \frac{\sqrt{\beta_i}}{\sqrt{M}} e^{-\jmath k R_i} e^{+\jmath k(j-1)d\cos(\phi_i)}, \;\; j = 1, ..., M, \qquad (1)$$

where β_i is the large-scale fading for user i, k is the wave number, R_i is the distance from user i to the array, d is the

[1]The following notation is used throughout the paper. Lowercase letters, bold lowercase and bold uppercase letters denote scalars, column vectors and matrices, respectively. The symbol $\mathbb{C}$ denotes complex numbers. The symbols $|\cdot|$ and $\|\cdot\|$ denote the absolute value and l^2-norm operators. The superscript ^{H} denotes conjugated transpose. The symbol $\boldsymbol{I}_M$ denotes the identity matrix of size M. A diagonal matrix with diagonal entries taken from $\boldsymbol{p}$ is denoted by $\text{diag}(\boldsymbol{p})$

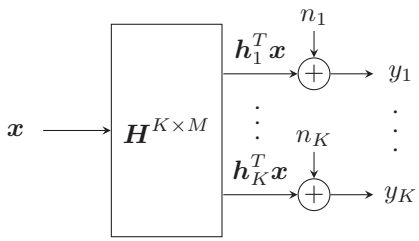

Fig. 1. The model of the downlink channel.

spacing between the elements, and ϕ_i specifies the direction of user i with respect to the array axis (see [8, Fig. 7.3 (b)]).

For further analysis, we use the spatial correlation between the channel vectors of user i and user j:

$$\rho_{ij} = \left| \frac{\boldsymbol{h}_i^H \boldsymbol{h}_j}{\|\boldsymbol{h}_i\| \|\boldsymbol{h}_j\|} \right|. \tag{2}$$

By replacing (1) in (2), ρ_{ij} becomes:

$$\rho_{ij} = \frac{1}{M} \left| \frac{\sin(Mk\frac{d}{2}\psi_{ij})}{\sin(k\frac{d}{2}\psi_{ij})} \right|, \tag{3}$$

where ψ_{ij} is:

$$\psi_{ij} = \cos(\phi_i) - \cos(\phi_j). \tag{4}$$

We omit the indices $_{ij}$ from ρ_{ij} and ψ_{ij} for notation simplicity for the rest of the paper. The spatial correlation ρ in (3) is a periodic function of ψ with the fundamental period of $T = \lambda/d$ (see Section 7.2.4 of [8] for more details).

The downlink Shannon capacity of a multi-user MIMO channel with K users is found by solving the following optimization problem [9]:

$$\begin{aligned} C = \max_{p_i, i=1,\ldots,K} & \log_2 \det\left(\boldsymbol{I}_M + \frac{1}{N_0}\boldsymbol{H}^H \text{diag}(\boldsymbol{p})\boldsymbol{H}\right), \\ \text{s.t.} & \sum_{i=1}^{K} p_i = P_{\text{tot}}, \end{aligned} \tag{5}$$

where N_0 is the variance for the AWGN at the users' receivers, $p_i, i = 1, ..., K$ are the power allocation coefficients, and P_{tot} is the total radiated power at the BS. The ϵ-outage capacity denoted by C_ϵ is defined in [8, Sec. 5.4.1] as the maximum rate of transmission with the outage probability less than ϵ. The 0.05-outage capacity is used in this paper as the performance metric. For a given FoV of ϕ_{FoV}, and a given inter-element spacing of d, we denote the 0.05-outage capacity by $C_{0.05}(d, \phi_{\text{FoV}})$.

III. Capacity Analysis

In this section, first, the downlink capacity is studied for a channel of two users as a function of ρ. Then, ρ is studied as a function of ψ, where we address the effects of d and FoV on this function. This reveals the effects of d and FoV on the downlink capacity, and consequently, the 0.05-outage capacity.

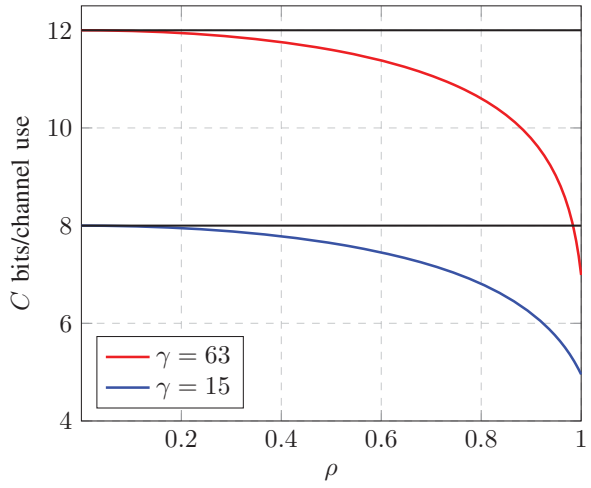

Fig. 2. The downlink capacity C over ρ for $\gamma = 15$ and 63, when the users have the same large-scale fading. The upper horizontal line shows $C^{\text{ortho.}}$ for $\gamma = 63$ and the lower horizontal line shows $C^{\text{ortho.}}$ for $\gamma = 15$.

A. Downlink Capacity vs. Spatial Correlation

Consider a channel $\boldsymbol{H}$ of two users with the same large-scale fading β and the spatial correlation of ρ among the users. The downlink capacity is found by solving the optimization problem in (5) using [10, eq. (6)] as:

$$C(\rho) = \log_2\left(1 + \frac{\beta P_{\text{tot}}}{N_0} + \frac{\beta^2 P_{\text{tot}}^2}{4N_0^2}(1-\rho^2)\right). \tag{6}$$

Equation (6) shows that the downlink capacity $C(\rho)$ is a decreasing function of ρ. The maximum downlink capacity denoted by $C^{\text{ortho.}}$ is found by:

$$C^{\text{ortho.}} = C(\rho = 0) = 2\log_2\left(1 + \frac{\beta P_{\text{tot}}}{2N_0}\right), \tag{7}$$

which is obtained when the users have orthogonal channel vectors. In this case, the signal to noise ratio (SNR) denoted by γ is:

$$\gamma = \frac{\beta P_{\text{tot}}}{2N_0}. \tag{8}$$

The effects of ρ on the achievable sum-rates of linear precoders are addressed in the literature [10]–[12]. The downlink capacity as a function of ρ is shown in Fig. 2 for two different SNRs when $\gamma = 15$ and 63. The upper horizontal line in Fig. 2, shows $C^{\text{ortho.}}$ for $\gamma = 63$ and the lower horizontal line shows $C^{\text{ortho.}}$ for $\gamma = 15$. As expected from (6), by increasing ρ, $C(\rho)$ decreases.

B. Spatial Correlation vs. ψ

By assuming a uniform distribution for ϕ_1 and ϕ_2 in the FoV of $[\phi_{\min}, \phi_{\max}]$ ($\phi_{\text{FoV}} = \phi_{\max} - \phi_{\min}$), the distribution of ψ can be found. A histogram of ψ is shown in Fig. 3 for an FoV of 120° ($\phi \in [30°, 150°]$). Note that the precision in the ϕ domain is 0.1°. For a better illustration, the histogram values in Fig. 3 are normalized to have a maximum of 1. The histogram of ψ shows that it is more probable to have small

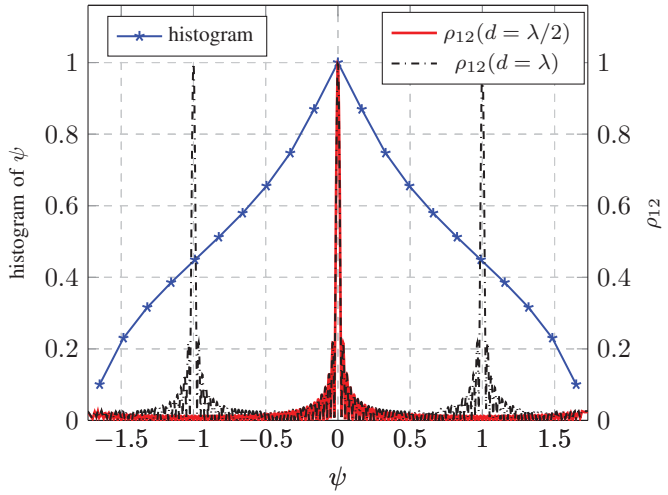

Fig. 3. A histogram plot of ψ along with ρ curves as a function of ψ for arrays with $d = \lambda/2$ and $d = \lambda$ for a fixed array size of 40λ in an FoV of 120°.

values of ψ (see the peak at $\psi = 0$). In addition, by increasing the absolute value of ψ, the histogram values decrease.

In addition to the histogram of ψ in Fig. 3, ρ is shown as a function of ψ for $d = \lambda/2$ and $d = \lambda$ for an array size of 40λ. Both the arrays have the same resolvability in the angular domain [8, Sec. 7.2.4] due to having the same array size. Figure 3 shows that the array with $d = \lambda/2$ has only one peak at $\psi = 0$ within the FoV of 120°. In contrast, the array with $d = \lambda$ has two other peaks at $\psi = -1$ and $\psi = 1$, which are the grating lobes. Having the grating lobes for the array with $d = \lambda$, results in a higher probability to have high values of ρ, or equivalently, a higher probability to have smaller $C(\rho)$ (see Fig. 2). This shows that the outage capacity for $d = \lambda$ must be smaller than $d = \lambda/2$.

C. Effects of d and FoV on The Outage Capacity

In this section, we study the effects of d and the FoV on ρ, and consequently, their effects on $C(\rho)$. For a given FoV, by increasing d, the number of grating lobes in the ρ function may increase, e.g., by increasing $d = \lambda/2$ to $d = \lambda$ as shown in Fig. 3. Therefore, increasing d may increase the probability of having a high ρ, and equivalently, increasing the probability of having a small $C(\rho)$. Consequently, for a given FoV, increasing d may result in a reduction in the 0.05-outage capacity. For a given FoV of ϕ_{FoV}, we propose to increase d, as long as $C_{0.05}(d, \phi_{\text{FoV}})$ does not reduce more than 1% compared to $C^{\text{ortho.}}$ as the following optimization problem:

$$\begin{aligned} d_{\text{opt.}} = \quad & \max \quad d \\ \text{s.t.} \quad & C_{0.05}(d, \phi_{\text{FoV}}) \geq 0.99\, C^{\text{ortho.}} \end{aligned} \tag{9}$$

Analyzing the effects of the FoV on $C_{0.05}(d, \phi_{\text{FoV}})$ is complicated. For a given d, reducing the FoV has two consequences. First, reducing the FoV limits the range of ψ. Thus, the number of grating lobes in the ρ function may reduce, e.g., see the ρ function for $d = \lambda$ in Fig. 3 when the FoV is reduced from 120° ($\psi \in [-\sqrt{3}, \sqrt{3}]$) to 60° ($\psi \in [-1, 1]$). Therefore, it is expected that reducing the FoV for a given d may improve the communication. Second, reducing the FoV increases the probability of having a certain ρ for the two users. For a large array size of $L >> \lambda$, and $\Delta\phi = |\phi_1 - \phi_2| \leq \lambda/(2L)$, the probability of having $\rho \in (2/\pi, 1)$ due to the peak at $\psi = 0$ is found as:

$$\Pr\left\{\rho \in \left(\frac{2}{\pi}, 1\right)\right\} = \Pr\left\{|\Delta\phi| < \frac{\lambda}{2L}\right\} \approx \frac{\frac{\lambda}{L}}{\phi_{\text{FoV}}}. \tag{10}$$

Equation (10) shows that reducing the FoV increases the probability of having a high ρ for a given d, which degrades the communication. Taking the two aforementioned consequences of limiting the FoV into account, it is not clear whether reducing the FoV may improve or degrade the communication. We study the effect of reducing the FoV on the outage capacity by simulations.

IV. Simulations

In this section, simulations are given to find $d_{\text{opt.}}$ for FoVs of 60° to 120°. Uniform linear arrays of isotropic radiators are considered with the same array size of 40λ. The users are uniformly distributed in a given FoV at the cell-edge (200 m far from the BS) to compare the worst-case scenarios for the arrays. The minimum angular separation of the users is assumed to be 0.001°. The center frequency of 30 GHz is assumed. Two SNR values are considered, i.e., $\gamma = 15$ and 63, which result in $C^{\text{ortho.}} = 8$ and 12 bits/channel use, respectively (see (7) and (8)). The radiated power at the BS is adjusted to have the same EIRP when reducing the number of elements.

In Fig. 4, $C_{0.05}(d, \phi_{\text{FoV}})$ is shown as a function of d for FoVs of 60° (solid blue) and 120° (dashed red) for $\gamma = 15$ and 63. For clarity, the other FoVs are not shown in Fig. 4. Based on (9), to find $d_{\text{opt.}}$, $C_{0.05}(d, \phi_{\text{FoV}})$ can be reduced to 7.92 and 11.88 bits/channel use for $\gamma = 15$ and 63, respectively (see the horizontal lines in Fig. 4). Eventually, for an FoV of ϕ_{FoV}, $d_{\text{opt.}}$ is found by finding the intersection of the horizontal lines and $C_{0.05}(d, \phi_{\text{FoV}})$. For FoVs of 60° to 120°, d can be increased to 1.14λ (see the red shaded area). For some FoVs and higher SNRs, d can be increased further. For instance, for FoV of 90° and $\gamma = 63$, $d_{\text{opt.}} = 1.29\lambda$ is obtained. In addition, Fig. 4 shows that reducing the FoV from 120° to 60° does not change $C_{0.05}(d, \phi_{\text{FoV}})$ considerably.

V. Conclusion

In this paper, the outage capacity is studied as a function of inter-element spacing and FoV for a given array size in LOS environments. It is shown for a given array size and a given FoV, one can increase the inter-element spacing considerably while achieving almost the same outage performance. For instance, for an array size of 40λ and FoVs of 60° to 120°, the inter-element spacing can be increased to more than 1.14λ. In addition, simulation results show that reducing the FoV from 120° to 60° does not change the outage performance considerably.

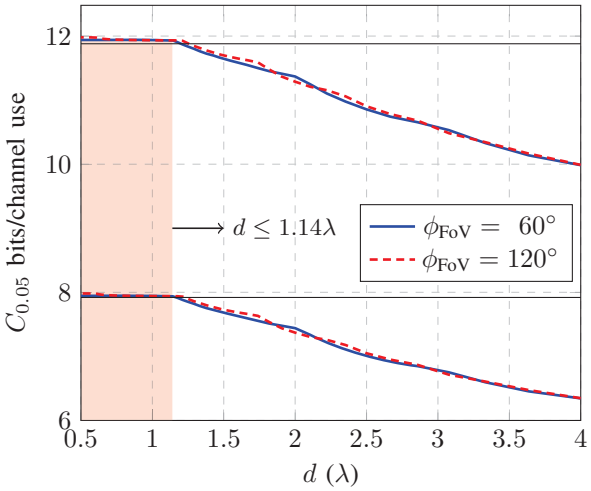

Fig. 4. $C_{0.05}(d, \phi_{\text{FoV}})$ as a function of d for $\phi_{\text{FoV}} = 60°$ (solid blue lines) and $120°$ (dashed red lines) for $\gamma = 15$ and 63 for an array size of 40λ. The upper horizontal line shows $0.99C^{\text{ortho.}}$ for $\gamma = 63$ and the lower horizontal line shows $0.99\, C^{\text{ortho.}}$ for $\gamma = 15$, which are used to find $d_{\text{opt.}}$. The shaded area shows the range of d ($d \leq 1.14\lambda$) when the outage performance is acceptable for FoVs of $60°$ to $120°$.

REFERENCES

[1] T. L. Marzetta, "Massive MIMO: An introduction," *Bell Labs Technical Journal*, vol. 20, pp. 11–22, Mar. 2015.

[2] H. Yang and T. L. Marzetta, "Max-min SINR dependence on channel correlation in line-of-sight massive MIMO," in *2017 IEEE Global Communications Conference (GLOBECOM)*, Dec. 2017, pp. 1–6.

[3] J. Flordelis, F. Rusek, X. Gao, G. Dahman, O. Edfors, and F. Tufvesson, "Spatial separation of closely-located users in measured massive MIMO channels," *IEEE Access*, vol. 6, pp. 40 253–40 266, 2018.

[4] Y. Aslan, J. Puskely, J. H. J. Janssen, M. Geurts, A. Roederer, and A. Yarovoy, "Thermal-aware synthesis of 5G base station antenna arrays: An overview and a sparsity-based approach," *IEEE Access*, vol. 6, pp. 58 868–58 882, 2018.

[5] N. Amani, A. A. Glazunov, M. V. Ivashina, and R. Maaskant, "Per-antenna power distribution of a zero-forcing beamformed ULA in pure LOS MU-MIMO," *IEEE Communications Letters*, vol. 22, no. 12, pp. 2515–2518, Dec. 2018.

[6] R. Janaswamy, "Effect of element mutual coupling on the capacity of fixed length linear arrays," *IEEE Antennas and Wireless Propagation Letters*, vol. 1, pp. 157–160, 2002.

[7] Shuangqing Wei, D. L. Goeckel, and R. Janaswamy, "On the asymptotic capacity of MIMO systems with fixed length linear antenna arrays," in *IEEE International Conference on Communications (ICC)*, May 2003, pp. 2633–2637.

[8] D. Tse and P. Viswanath, *Fundamentals of Wireless Communication*. New York, NY, USA: Cambridge University Press, May 2005.

[9] P. Viswanath and D. N. C. Tse, "Sum capacity of the vector Gaussian broadcast channel and uplink-downlink duality," *IEEE Transactions on Information Theory*, vol. 49, no. 8, pp. 1912–1921, Aug. 2003.

[10] X. Gao, O. Edfors, F. Rusek, and F. Tufvesson, "Linear pre-coding performance in measured very-large MIMO channels," in *2011 IEEE Vehicular Technology Conference (VTC Fall)*, Sep. 2011, pp. 1–5.

[11] A. Farsaei, F. Willems, A. Alvarado, and U. Gustavsson, "A reduced-complexity linear precoding strategy for massive MIMO base stations," in *2018 25th International Conference on Telecommunications (ICT)*, Jun. 2018, pp. 121–126.

[12] A. Farsaei, A. Alvarado, F. M. J. Willems, and U. Gustavsson, "An improved dropping algorithm for line-of-sight massive MIMO with max-min power control," *IEEE Communications Letters*, preprint, Apr. 2019.